

Article

Modified Vermiculite as Adsorbent of Hexavalent Chromium in Aqueous Solution

Celia Marcos ^{1,*}, Valeria Medoro ¹ and Alaa Adawy ²

¹ Departamento Geología e Instituto de Química Organometálica “Enrique Moles”, Universidad Oviedo, Jesús Arias de Velasco s/n, 33005 Oviedo, Spain; valeria.medoro@student.unife.it

² Laboratory of High-Resolution Transmission Electron Microscopy, Institute for Scientific and Technological Resources, Edificio Severo Ochoa s/n, Campus de El Cristo, 33006 Oviedo, Spain; hassanalaa@uniovi.es

* Correspondence: cmarcos@uniovi.es; Tel.: +34-9-8510-3100

Received: 23 July 2020; Accepted: 21 August 2020; Published: 24 August 2020



Abstract: The aim of this study was to investigate the efficiency of removing Cr⁶⁺ from aqueous solutions using two exfoliated vermiculite: (1) heated abruptly at 1000 °C and (2) irradiated with microwave radiation. The effects investigated were contact time, adsorbate concentration and initial Cr⁶⁺ concentration. The adsorption with both exfoliated vermiculites was well described by the DKR isotherm, indicative of a cooperative process and with the pseudo second order kinetic model. The K_d value for the two exfoliated vermiculites was similar, 0.2×10^{10} µg/Kg. The maximum adsorption capacity of Cr⁶⁺ with thermo-exfoliated vermiculite, 2.81 mol/g, was much higher than with microwave irradiated vermiculite, 0.001 mol/g; both values were obtained with 0.5 g of vermiculite in contact with distilled water enriched with 1 ppm of Cr⁶⁺ for 24 h. Factors such as ion chemistry, the solution pH and ionic strength, influence the values of capacity, adsorption energy and initial adsorption rate values of the exfoliated vermiculite. In addition, these values depended on the exfoliation process, being the adsorption capacity highest with abrupt heating of vermiculite, while the adsorption energy and rate values showed just a slight increase with microwave irradiation. This aspect is important to select the most suitable vermiculite modification treatment to use it as an adsorbent.

Keywords: vermiculite; Cr⁶⁺ adsorption; thermo-exfoliation; microwaves

1. Introduction

There are numerous materials used as Cr⁶⁺ adsorbents in aqueous solution using procedures such as chemical precipitation, evaporation, reverse osmosis, ion exchange or adsorption [1–10]. On the other hand, the usage of thermo-exfoliated vermiculite can be considered as a cheap and good solution for this environmental problem owing to its high specific surface area and ion exchange capacity while it does not get wet easily in aqueous solution in spite of its ability to absorb a relatively big amount of water. In this work, the adsorption of Cr⁶⁺ in aqueous solution by exfoliated vermiculite at high temperature and vermiculite irradiated with microwaves has been investigated because to our knowledge we could not find any previous attempts that reported the ability of using thermo exfoliated vermiculite to remove Cr⁶⁺ from aqueous solutions. This is despite the fact that we successfully used the same exfoliated vermiculite to remove Cr³⁺ and Ni²⁺ from aqueous solutions [11,12].

Vermiculite is a hydrated aluminum, iron and magnesium silicate, belonging to the 2:1 group of the phyllosilicate mineral subclass. It is similar in appearance to micas, with laminar habit and perfect exfoliation (001); its color is variable in brown, yellowish green or brownish green tones; and with low density (2.4–2.7 g/cm^{−3}). These characteristics are derived from its structure that is composed of an octahedral layer O between two tetrahedral T layers, constituting the T-O-T sheet. The T layer is formed by pseudo-hexagonal rings of SiO₄ tetrahedra sharing three of their four oxygens with adjacent

tetrahedra. The O layer consists of divalent cations (Mg^{2+}), coordinated with 4 O^{2-} ions and 2 OH^{-} groups. The existence of isomorphic substitutions (Al^{3+} and, occasionally, Fe^{3+} instead of Si^{4+} in layer T; Al^{3+} , Fe^{3+} , Fe^{2+} or Ti^{4+} , among others, instead of Mg^{2+} in layer O) leads to the appearance of electric charge on the surface of the TOT sheet that is compensated by the presence of cations in the inter-layer space; mostly Mg^{2+} , although there may also be small amounts of Ca^{2+} or Na^{+} . The structure consists of two T-O-T sheets joined by hydrated cations located in the so-called inter-layer space. Vermiculite can undergo dehydration-hydration processes that depend on temperature, pressure, chemical composition, particle size and relative humidity [13–17]. The state of hydration of vermiculite was defined by the number of layers of water (0, 1 and 2) in the inter-layer space resulting in phases with different states of hydration namely: 0—WLHS, with zero layers of water; 1—WLHS, with one layer of water and 2—WLHS, with two layers of water [18].

Commercial or industrial vermiculite consists of interstratified diverse of mica, mica/vermiculite and a combination of phases corresponding to the different hydration states described above. These vermiculites are characterized by their industrial and technological applications. In addition, these commercial vermiculites exfoliated might be an optimal product for the adsorption of substances of environmental impact, like aromatic compounds, toxic metals or pesticides, due to their high expansive capacity and high specific surface area [19,20].

Chromium is a heavy metal, with a density of 5.0×10^6 mg/L, low solubility of its oxides and hydrates and different oxidation states that vary from -2 to $+6$ [5]. Chromium can be released from the alteration of rocks, but most of it results from anthropogenic processes, for example from the steel industry, galvanizing companies, chemical industries (catalysts, fungicides and dyes), medicine, photography and lithography, abrasive production, etc. Since 2006 the World Health Organization designates as reference values for total chromium 0.05 mg/L in drinking water and 0.1 mg/L in the soil [9]. The most common forms of Cr are Cr^{3+} and Cr^{6+} . The latter, with an ionic radius of 0.52 Å, and it is the most toxic form in which this element can appear. Cr^{6+} is known to be highly soluble in water, mobile, and there are very serious water pollution incidents that were reported when effluents containing chromium compounds have been evacuated in rivers. The danger of Cr^{6+} is due to bioaccumulation in the food chain and its harmful effects on health, since it has great mobility in the soil and in the aquatic system [1].

The objective of this research was to investigate the efficiency of the adsorption of Cr^{6+} in aqueous solution by a commercial vermiculite exfoliated with two different treatments, thermally at high temperature and irradiated with microwave radiation.

2. Materials and Methods

The vermiculite of this work came from China (CHG). It was in the form of small packets of a green color with different tints, with maximum dimensions of 1–2 mm in diameter and 0.5–1 mm in thickness. According to the classification of commercial vermiculites proposed by [20], it would belong to type-2.

The sample was manually cleaned through removing all mineral particles other than vermiculite with the aid of a magnifying glass and tweezers. This step was followed by the exfoliation of the vermiculite with (1) abruptly heating in an oven at 1000 °C for 1 min, and (2) with microwave irradiation in a microwave oven (SHARP R64sT) working at 2.45 GHz of frequency with 800 W of energy for 25 s. The expansibility (density of the raw sample/density of the expanded sample), was measured by the change of the apparent density. A known volume of sample was weighed and expanded. The apparent volume was measured by tipping the loose fragments into a measuring glass cylinder without compactation. For simplicity the exfoliated samples with high temperature and with microwave radiation were encoded CHGE-H and CHGE-MW, respectively.

The chemical composition of the CHG, CHGE-H and CHGE-MW vermiculites has been determined by X-ray fluorescence (XRF) with an X-ray fluorescence spectrometer PW2540 equipped with a rhodium anode (Rh) tube with 4 kW of power, five analyzer crystals (Fli 200, Fli 220, Pe, Ge and Px1) and

three detectors: xenon sealing, scintillation and gas flow. In the quantitative analysis, a calibration for geological samples was available, with international reference standards. The major elements determined were: Al_2O_3 , P_2O_5 , K_2O , CaO , SiO_2 , TiO_2 , MnO_2 , Fe_2O_3 , MgO , Na_2O and as trace elements: V, Cr, Co, Ni, Cu, Zn, Ba, Nb, Rb, Sr, Y, Zr, U, Th, Pb, S. To analyze the major elements, beads from the CHG, CHGE-H and CHGE-MW samples were prepared by fusion with a Quielab pearl. For the minor elements, a tablet of the CHG (from the CHGE-H and CHGE-MW samples it was impossible to prepare) was prepared with a Herzog press.

The specific surface area of CHG, CHGE-H and CHGE-MW was obtained using N_2 physisorption analysis with an ASAP 2020 equipment (Micromeritics, Norcross, GA, USA) under the following conditions: Nitrogen adsorption at 77.35 K, with σ_m (N_2) assumed to be 0.162 nm^2 (based on the assumption of a closed-packed monolayer). Unrestricted evacuation of 30.0 mm Hg, vacuum pressure of $10 \mu\text{m Hg}$, evacuation time of 1 h, and the temperature of sample evacuation prior to N_2 adsorption measurements was 22° . The data were recorded with equilibration times (p/p_0 between 0.001 and 1.000) between 50 s and 25 s and a minimum equilibrium delay of 600 s at $p/p_0 \geq 0.995$. Specific surface area was determined by using a mathematical description of the adsorption isotherms with the software of the equipment.

For the adsorption investigations a chromium standard solution Cr^{6+} of (NIST) = $1000 \pm 10 \text{ mg L}^{-1}$ in diluted NaOH was used. All the following experiments were carried out with CHGE-H and CHGE-MW in duplicate. For CHGE-H sample, an aqueous solution of chromium was prepared from a standard solution of 1000 mg/L of Cr^{6+} through dilution in distilled water down to 100 mL with 1 ppm of Cr^{6+} , the pH of which was measured, and the concentration was verified using ICP-MS. Afterwards, seven aqueous solutions of 10 mL each were prepared in polypropylene tubes, enriched with 1 ppm of Cr^{6+} . After measuring the pH of each tube, 0.3 g of CHGE-H sample were put well immersed in the solution for 2, 4, 8, 14, 24, 48 and 72 h. In order to study the effect of chromium concentration on its adsorption, other six aqueous solutions of 10 mL each were prepared in polypropylene tubes with Cr^{6+} of 0.125, 0.25, 0.50, 0.75, 1 and 2 ppm. After pH measurement, 0.5 g of CHGE-H sample was well immersed into each tube. To study the effect of mass, another series of six aqueous solutions of 10 mL each enriched with 1 ppm of Cr^{6+} were prepared in polypropylene tubes into which increasing masses of 0.1, 0.2, 0.3, 0.5, 0.7 and 1 g of CHGE-H were well immersed. The contact time used in the adsorption experiments related to the adsorbent mass and concentration of the adsorbate was 24 h, like that was previously adopted for the experiments with Cr^{3+} and the same vermiculite [11]. The same procedure was carried out with the CHGE-MW microwave irradiated samples. The exfoliated samples contacted with Cr^{6+} were labeled as CHGE-H-Cr and CHGE-MW-Cr, respectively. After all the above investigations, the treated samples were filtered from the solution and dried out. The effect of ionic strength on the adsorption with the sample CHGE-H was investigated at 0–4.0 mol/L NaCl salt concentrations at 25°C and constant initial Cr^{6+} concentration of 1 ppm. This sample was labeled as CHGE-H-Cr-ClNa.

The inductively coupled plasma mass spectrometry (ICP-MS) with the HP 700 Agilent apparatus was used to analyze the content of chromium cation. The Cr^{6+} content in the samples was determined by diluting the samples in 2% HNO_3 and using Ga for calibration.

The adsorbed amount of Cr^{6+} at equilibrium conditions K_d ($\mu\text{g/Kg}$) was calculated by:

$$K_d = \frac{(C_i - C_e)}{m} V, \quad (1)$$

where C_i and C_e are the initial and equilibrium concentrations, respectively and V and m are the liquid volume and the weight of adsorbent applied, respectively.

The mineral phases of the CHG, CHGE-H, CHGE-MW, CHGE-H-Cr and CHGE-MW-Cr samples were determined by X-ray diffraction (XRD) using a PHILIPS X 'PERT PRO diffractometer (PHILIPS, Amsterdam, The Netherlands). The machine settings were 40 mA and 45 kV (Cu- $\text{K}\alpha$ radiation; $\lambda =$

1.5418 Å), 2θ range 5–35 degrees, 2θ step scans of 0.007° and a counting time of 1 s per step. Aluminum sample holder was used for the powdered sample (0.5 g).

Adsorption data were described by adsorption isotherms, mathematical models that describe the distribution of the adsorbate species among liquid and adsorbent, based on a set of assumptions that are mainly related to the heterogeneity/homogeneity of adsorbents, the type of coverage and possibility of interaction between the adsorbate species. The linear forms of the Langmuir [21], Freundlich [22] and Dubinin–Kaganer–Radushkevich (DKR) [23] isotherms models were used to determine the isotherm parameters.

The linear expression of Langmuir isotherm:

$$\frac{1}{q_e} = \left[\frac{1}{q_m K_L} \right] \frac{1}{C_e} + \frac{1}{q_m}, \quad (2)$$

The linear expression of Freundlich isotherm:

$$\log q_m = \log K_F + \frac{1}{n} \log C_e, \quad (3)$$

where K_L (L/mg) and q_m (mg/g), maximum adsorption capacity, are constants related to the energy of adsorption and energy or net enthalpy of adsorption, respectively; K_F (mg/g) and n are the constants, which measure the adsorption capacity and intensity and an indication of how favorable the adsorption processes, respectively.

The DKR equation has the form:

$$\ln C_{ads} = \ln X_m - \beta \varepsilon^2, \quad (4)$$

where C_{ads} is the number of metal ions adsorbed per unit weight of adsorbent (mol/g), X_m (mol/g) is the maximum adsorption capacity, β (mol^2/J^2) is the activity coefficient related to mean adsorption energy, and ε is the Polanyi potential, which is equal to:

$$\varepsilon = RT \ln \left(1 + \frac{1}{C_e} \right), \quad (5)$$

where R is the gas constant (8.314 kJ/mol K) and T is the temperature (K). The saturation limit X_m may represent the total specific micro-pore volume of the sorbent. The slope of the plot of $\ln C_{ads}$ versus ε^2 gives β (mol^2/J^2) and the intercept yields the adsorption capacity, X_m (mol/g).

The adsorption energy was calculated using the following relationship:

$$E = \frac{1}{\sqrt{-2\beta}}, \quad (6)$$

Adsorption kinetic studies were carried out to describe the metal adsorption rate, which in turn governs the residence time of the adsorption reaction and also the efficiency of the adsorption process. The linearized forms of pseudo-first-order and pseudo-second-order equations [24] were used:

$$\log(q_e - q_t) = \log q_e \text{ calc} - \frac{k_1}{2.303} t, \quad (7)$$

$$\frac{1}{q_t} = \frac{1}{k_2 q_e^2 \text{ calc}} + \frac{t}{q_e \text{ calc}}, \quad (8)$$

where q_e is the metal adsorbed at equilibrium (mg/g), q_t is the amount of the metal adsorbed (mg/g) at any time t , k_1 is the first-order rate constant. The first-order rate constants k_1 and $q_e \text{ calc}$ were determined from the slopes and intercept of plots of $\log(q_e - q_t)$ versus t at different metal concentration. The

second-order rate constants (k_2) and q_e cal were determined from the slope and intercept of the plot obtained by plotting t/q_t versus $t \cdot kq_e^2$ (mg/g min) can be regarded as the initial adsorption rate as $t \rightarrow 0$.

3. Results

The expansibility for CHGE-H and CHGE-MW was similar, 7.3 and 7.4, respectively. In Figure 1 the aspect of CHGE-H (Figure 1a) and CHG-MW (Figure 1a) is shown.

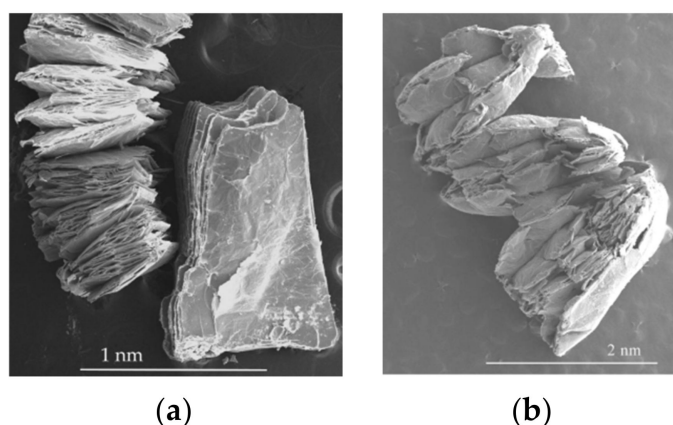


Figure 1. Exfoliated vermiculites: (a) abruptly at 1000 °C, CHGE-H sample and (b) microwave irradiation, CHGE-MW.

The major elements percentages expressed in oxides and analyzed by XRF (Table 1) were similar for CHG and CHG-MW, the same as the loss on ignition value (L.O.I.). In CHGE-H the percentages were higher and the L.O.I. was much lower. L.O.I. is mainly due to evaporation of water when the sample is heated to high temperatures.

Table 1. Major elements percentages expressed in oxides.

Element Oxides	Weight %		
	CHG	CHGE-H	CHGE-MW
SiO ₂	37.14	42.30	37.31
Al ₂ O ₃	11.60	13.22	11.68
Fe ₂ O ₃	5.23	5.86	5.10
MnO	0.03	0.04	0.03
MgO	23.63	26.43	23.47
CaO	1.51	1.29	1.32
Na ₂ O	1.40	1.58	1.42
K ₂ O	3.92	4.58	3.62
TiO ₂	1.25	1.38	1.20
P ₂ O ₅	0.00	0.01	0.00
L.O.I.	14.08	3.31	14.52
TOTAL	99.79	99.99	99.67

L.O.I.: Loss on ignition value.

The minor elements detected were Cr and Ba with percentages of 0.17423 and 0.24772, respectively, and the percentage of the rest of the elements (V, Co, Cu, Zn, Ga, As, Se, Rb, Sr, Zr, Nb, Ag, Cs, Tl, Pb, U) detected was less than 0.04.

The specific surface area of the CHGE-H sample, 10.7560 ± 0.0318 m²/g, was twice that of the untreated CHG sample, 5.2605 ± 0.0770 m²/g, and the microwave irradiated CHGE-MW sample, 4.1111 ± 0.0917 m²/g.

The weight of the vermiculites before and after the adsorption experiment was similar.

The pH of the distilled water solution enriched with 1 ppm of Cr^{6+} was 7.3. After the contact time of the samples with the solution, between 2 and 72 h, the pH varied between 7 and 8 for CHGE-H and approximately 7.4 for CHGE-M. Depending on the mass of the samples, between 0.1 and 1 g, the pH ranged between 7.0 and 7.9 for CHGE-H and CHGE-MW. Finally, with the concentration in ppm of Cr^{6+} , between 0.1 and 2, the pH varied between 7.6 and 10.2 before introducing the CHGE-H and CHGE-MW and between 7.6 and 9.5 after immersing the CHGE-H in the solution 24 h and filtering it.

Tables 2–4 show the ICP-MS (ppm) of Cr^{6+} adsorbed in the distilled water solution with Cr^{6+} in contact with CHGE-H and CHGE-MW, respectively. There was no apparent trend in the Cr^{6+} adsorption when related to the contact time at constant mass and concentration of the CHGE and Cr^{6+} -solution enrichment, respectively (Table 2).

Table 2. The variation of Cr^{6+} (%) adsorption by 0.3 g of CHGE with the contact time.

Contact Time (h)	% Cr^{6+} Adsorbed by CHGE-H	% Cr^{6+} Adsorbed by CHGE-MW
2	68.274 (0.235)	26.47 (0.130)
4	58.980 (0.376)	20.87 (0.271)
8	56.660 (0.024)	26.82 (0.124)
16	67.300 (0.475)	26.07 (0.365)
24	62.260 (0.074)	20.02 (0.214)
48	63.860 (0.395)	21.16 (0.270)
72	67.300 (0.354)	19.96 (0.163)

The values of Cr^{6+} adsorbed by increasing masses of CHGE in contact with 1 ppm (Cr^{6+}) enriched solution for 24 h are presented in Table 3. As the data reveal, Cr^{6+} adsorption decreases with the increase in the tested mass in a trend that was contradicted for one value (0.5 g).

Table 3. The variation of Cr^{6+} (%) adsorbed by increasing masses of CHGE in contact with 1 ppm Cr^{6+} enriched solution for 24 h.

CHGE Mass (g)	% Cr^{6+} Adsorbed by CHGE-H	% Cr^{6+} Adsorbed by CHGE-MW
0.1	61.49 (0.001)	77.21 (0.064)
0.2	53.47 (0.064)	50.23 (0.312)
0.5	64.40 (0.107)	37.64 (0.133)
0.7	41.95 (0.081)	39.15 (0.008)
1.0	43.14 (0.264)	50.89 (0.164)

From the experiments done by immersing 0.5 g of CHGE-H and CHGE-MW, respectively, into solutions with increasing concentrations of Cr^{6+} incubated for 24 h, a decrease in Cr^{6+} adsorption by CHGE-H was detected with the increase in the Cr^{6+} initial concentration up to 0.75 ppm and then the adsorption increased at higher concentrations up to 1 ppm (Table 4). With the CHGE-MW sample a different behavior is observed, firstly the adsorption increases with increasing concentration up to 1 ppm and then decreases.

Table 4. Cr^{6+} percentage adsorbed by 0.5 g of CHGE in contact with the distilled water solution for 24 h, as a function of the concentration (ppm) of Cr^{6+} .

Concentration (ppm) of Cr^{6+}	% Cr^{6+} Adsorbed by CHGE-H	% Cr^{6+} Adsorbed by CHGE-MW
0.10	94.958 (0.725)	49.6 (0.625)
0.25	84.999 (1.097)	55.0 (0.992)
0.50	80.769 (1.955)	61.5 (2.010)
0.75	70.437 (9.316)	60.6 (0.775)
1.00	89.244 (2.535)	60.0 (1.446)
2.00	99.200 (0.000)	49.6 (0.334)

The XRD patterns of the samples are in Figure 2. CHG shows the presence of vermiculite with 2 layers of water at 14.68 Å (2-WLHS) and vermiculite with 1 layer of water at 11.15 Å (1-WLHS) [18] (JCPDS card 16-613); hydrobiotite with the most characteristic reflection at 12.69 Å (JCPDS card 13-465); mica (biotite, phlogopite or muscovite) with the reflection at 10.11 Å, as the most characteristic. The XRD patterns of the CHGE-H and CHGE-H-Cr in contact with the solution enriched with 1 ppm Cr^{6+} , respectively, are similar and correspond to phlogopite (JCPDS card 6-263). The CHGE-MW and CHGE-MW-Cr samples are similar to the starting sample CHG.

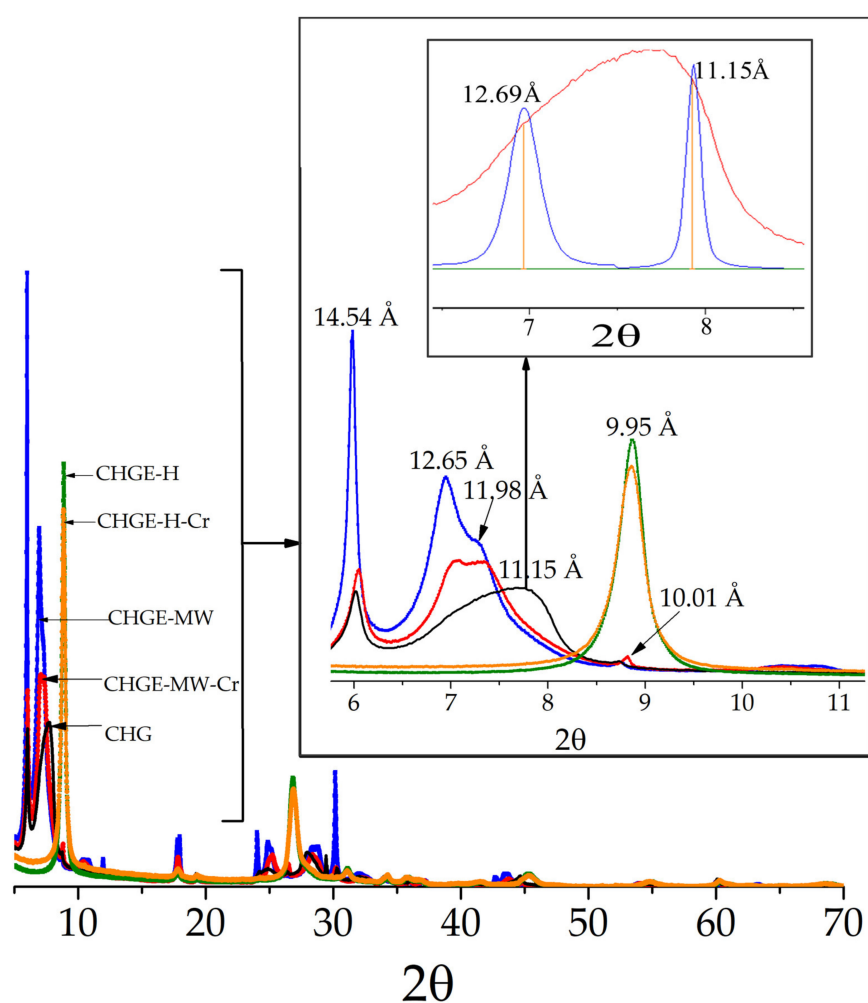


Figure 2. XRD patterns of the samples.

The linearized isotherm model that best fits the CHGE-H-Cr and the CHGE-MW-Cr samples is that of the DKR isotherm (Figure 3), since its correlation coefficients R^2 were the higher in both samples. The Langmuir, Freundlich and DKR parameters for CHGE-H and CHGE-MW from the adsorption isotherms of Cr^{6+} are in Table 5.

Gibbs free energy change (ΔG°) was calculated to be 0.297 KJ/mol for CHGE-H-Cr and -0.550 KJ/mol for CHGE-MW-Cr.

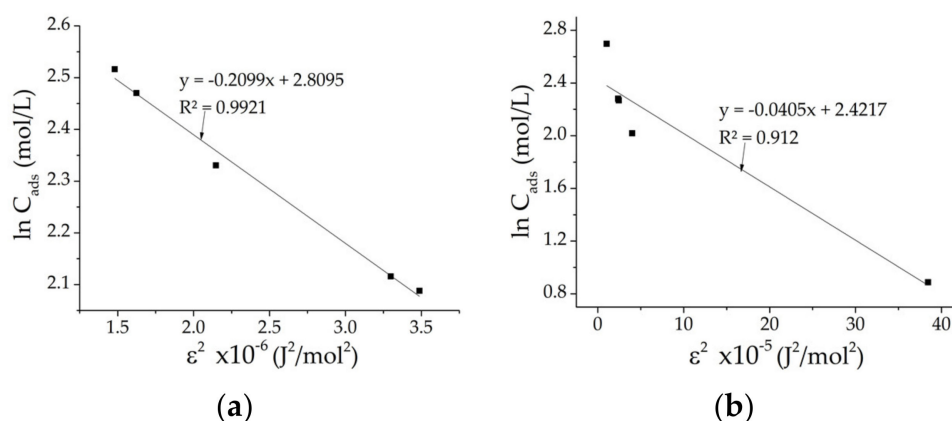


Figure 3. Linearized isotherms of DKR (a) for CHGE-H and (b) for CHGE-MW.

Table 5. DKR parameters for CHGE-H-Cr and CHGE-M-Cr.

Parameters	CHGE-H-Cr			CHGE-MW-Cr		
	Langmuir	Freundlich	DKR	Langmuir	Freundlich	DKR
K_L (L/mg)	-0.38	-	-	0.00	-	-
q_m (mg/mg)	-1.29	-	-	0.00	-	-
K_F	-	0.26	-	-	0.001	-
n	-	-1.13	-	-	-0.004	-
X_m (mol/g)	-	-	2.81	-	-	0.001
β (mol ² /J ²)	-	-	-0.21	-	-	-0.0002
E (KJ/mol)	-	-	0.002	-	-	0.047
R^2	0.958	0.989	0.992	0.783	0.922	0.912

The correlation coefficients values, R^2 , obtained from the linearized pseudo-first-order and pseudo-second-order equations indicate that the kinetic model that best fits both samples, CHGE-H-Cr and CHGE-MW-Cr, is the second (Figure 4). The parameters of these models for both samples are in Table 6.

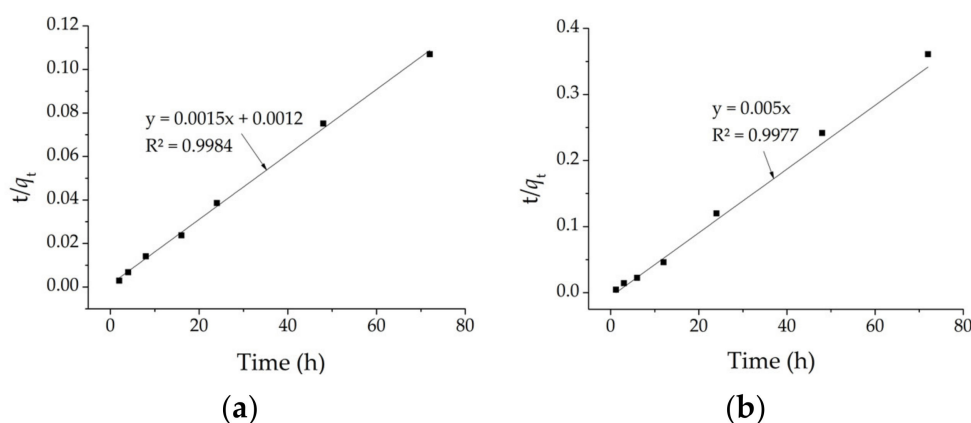


Figure 4. Representation of the linearized pseudo-second-order equation for CHGE-H-Cr (a) and CHGE-MW-Cr (b) samples.

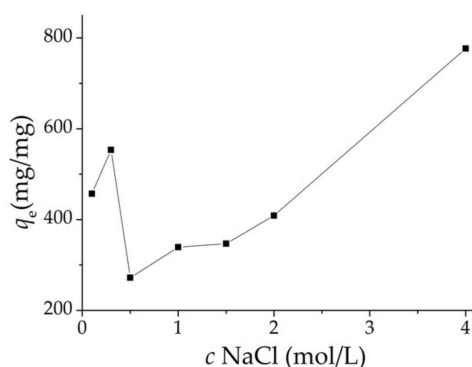
Table 6. Pseudo-second-order parameters for CHGE-H-Cr and CHGE-MW-Cr.

Parameters	CHGE-H-Cr		CHGE-MW-Cr	
	Pseudo-First-Order	Pseudo-Second-Order	Pseudo-First-Order	Pseudo-Second-Order
q_e (mg/g)	1.79	-	1.53	-
K_1 (h^{-1})	0.06	-	0.03	-
K_2 (h^{-1})	-	0.002	-	0.005
q_e (mg/g)	-	0.001	-	-0.006
R^2	0.337	0.998	0.020	0.984

The initial adsorption rate for CHGE-H-Cr and CHGE-MW-Cr, calculated from the from the product $k_2 \cdot q_e^2$, was 0.2×10^{-8} mg/g.h.

Two steps of adsorption decreasing are observed as the Cr^{6+} -vermiculite contact time increases; the first occurs in the first 8 h and the second occurs between the 16 and 24 h. In addition, other two steps of adsorption increasing are observed as the metal-vermiculite contact time increases; one between 8 and 16 h and the other after 24 h.

The effect of the ionic strength on the adsorption of Cr^{6+} onto the adsorbent is shown in Figure 5, while the NaCl concentrations increased from 0 to 0.3 mol/L, the adsorption amount of Cr^{6+} increased from 0.46 mg/mg to 0.55 mg/mg. Afterwards, the adsorption amount of Cr^{6+} decreased with the increase in NaCl from 0.3 to 0.5 mol/L. Thereafter, Cr^{6+} adsorption again increased with increasing NaCl concentrations. When the NaCl concentrations reached 4.0 mol/L, the adsorption amount of Cr^{6+} reached 0.78 mg/mg. The result indicated that the CHGE-H-Cr sample adsorbed a considerable amount of Cr^{6+} even at strong ionic strength.

**Figure 5.** Effect of ionic strength on the adsorption of Cr^{6+} onto the CHGE-H sample.

4. Discussion

The transformation of CHG vermiculite after heating it at 1000 °C for 1 min at phlogopite could be due to the high potassium content of the sample, dehydration and structural rearrangement as a consequence of the high temperature used [25]. The exfoliated vermiculite enriched in Cr^{6+} , CHGE-H-Cr, did not undergo any transformation, except a slight decrease in the intensity of the reflections, as there was no hydration or dehydration [25], corroborated with the fact that the weight of the vermiculites before and after the adsorption experiments was the same, contrary to what happened with the exfoliated vermiculite in contact with synthetic seawater enriched in Cr^{3+} [11]. Vermiculite CHG after microwave irradiation, CHGE-MW, underwent physical change (textural and color) and loss of crystallinity and order but no phase change. The cause would be that it lost little water (the L.O.I. was similar to the untreated vermiculite CHG) and as a consequence its specific surface area was similar to the CHG sample. The exfoliated vermiculite enriched in Cr^{6+} , CHGE-MW-Cr, remained as CHGE-MW, with a slight decrease in the intensity of the reflections.

The adsorption of Cr^{6+} by CHGE-H was dependent on the initial concentration, as it has been seen before. Such adsorption was very fast at the beginning since there were enough active sites that

could be easily occupied. As the concentration increased the adsorption decreased, until the active sorption sites could no longer accommodate Cr^{6+} due to saturation [26,27]. Afterwards, this process was inverted when Cr^{6+} left the active sites to return to the solution leaving out some active sites to be occupied by Cr^{6+} . In the CHGE–MW, the concentration increased and the adsorption decreased until 1 ppm of Cr^{6+} when the saturation occurred.

The DKR model fitted the experimental data best by linear analysis suggesting that the adsorption process would be cooperative (physical and ion diffusion), as also happened with the adsorption of Cr^{3+} and Ni^{2+} in synthetic seawater by the same exfoliated vermiculite [11,12].

The negative ΔG° value indicated thermodynamically feasible and spontaneous nature of the adsorption of CHGE–MW–Cr sample, while for CHGE–H–Cr the positive ΔG° value indicated that the process was not spontaneous. This difference seems to be related to the exfoliation product used as an adsorbent; in both cases they are similar in texture but different in relation to the phases of which they are composed.

Table 7 shows the adsorbed amount of Cr^{6+} at equilibrium conditions, the maximum adsorption capacity (X_m), the adsorption energy (E) and the initial Cr^{6+} adsorption rate obtained in the present study, in distilled water, compared with those of Cr^{3+} and Ni^{2+} obtained with the same exfoliated vermiculite by [11,12], in synthetic seawater.

Table 7. Comparison of Cr^{6+} adsorbed values, maximum adsorption capacity (X_m), adsorption energy (E) and initial Cr^{6+} adsorption rate obtained in this research with CHGE–H and CHGE–MW in distilled water with those obtained by [12] for Cr^{3+} and Ni^{2+} with CHGE–H in synthetic seawater.

Adsorbed Ion	Cr^{6+}		Cr^{3+}	Ni^{2+}	
	Treatment	Microwave Irradiation	Abrupt Heating at 1000 °C		
K_d ($\mu\text{g}/\text{Kg}$)		0.22×10^{10}	0.22×10^{10}	0.743×10^5	1.539×10^5
X_m (mol/g)		0.001	2.81	3.26	3.13
E (KJ/mol)		0.047	0.002	0.003	0.003
Initial Adsorption Rate (mg/g-h)		1.5×10^{-8}	0.2×10^{-8}	2×10^{-8}	2×10^{-8}

The fact that the X_m was higher in CHGE–H–Cr sample than in CHGE–MW–Cr sample and the E and the initial Cr^{6+} adsorption rate was lower could lie in the exfoliation treatment type because it influences the resulting product specific surface area. The adsorption capacity of thermally treated vermiculite, double than that irradiated by microwave irradiation, is mainly due to in the first case the resulting product (mica) was expanded and exfoliated, and in the second one (mixture of vermiculite and hydrobiotite with a little mica) was more expanded than exfoliated. As a result, the fresh exfoliated and expanded surface of mica has a large number of reactivity sites, which leads it have outstanding adsorption compared to the mixture of vermiculite, hydrobiotite and mica. This aspect is important to select the most suitable vermiculite modification treatment to use it as an adsorbent.

Moreover, the K_d , X_m , E and the initial adsorption rate values with Cr^{6+} were lower than with Cr^{3+} and Ni^{2+} could be attributed to the ion chemistry, to the higher pH of the synthetic seawater (8.5) in relation to the distilled water (7) and to the ionic strength.

When comparing the capacity of vermiculite to adsorb Cr^{6+} to other adsorbents it becomes clear that thermo–exfoliated vermiculite remains as a viable treatment option due to its high adsorption capacity, availability and low cost (Table 8). The adsorption capacity of Chinese vermiculite thermo–exfoliated is higher than that of pomace, sugarcane bagasse, natural clinoptilolite and Indian vermiculite, slightly lower than carbon slurr and carbon–microsilica and vermiculite from Palabora. At pH values lower than 6, Cr^{6+} removal efficiency by CHGE would probably increase because soluble hydroxylated complexes of the chromium would not form and would not compete for the active sites, and as a consequence, the retention would increase [28].

Table 8. Comparison of adsorption capacity of Chinese vermiculite thermoexfoliated for Cr⁶⁺ with that of different adsorbents. Note: Adsorption capacity values have been recalculated for an initial Cr⁶⁺ concentration of 1 ppm.

Adsorbents	Specific Surface Area (m ² /g)	Adsorption Capacity (mol/g)	pH	Reference
Carbon slurr	-	2.93	2	[3]
Pomace	1	1.99	-	[29]
Sugarcane bagasse	-	0.52	2	[2]
Carbon–microsilica	51	3.63	5–6	[7]
Natural Clinoptilolite	60.4	2.29	2	[9]
Palabora vermiculite	-	4.47–5.75	1.5	[6]
Turkish vermiculite	-	67.7	1.5	[30]
Indian vermiculite	-	0.5 and lower	-	[1]
Thermo–exfoliated vermiculite (China)	10.8	2.81	7	this paper

From all the available water treatment techniques, adsorption is generally preferred for the removal of heavy metal ions due to its high efficiency, easy handling, availability of different adsorbents and cost effectiveness [31–33]. Although this research has been carried out under controlled laboratory conditions, it is necessary to optimize the method using pH lower than that used in the present investigation to check if the adsorption time decreases. In addition, as our results indicate, the increase in concentration or mass of the exfoliated vermiculites does not increase the adsorption efficiency and this ensures that this treatment “less is more”. Moreover, it would be convenient to study the competitive adsorption of Cr⁶⁺ and other ions such as Ni²⁺, and finally to design an adequate adsorption tank.

The decrease of adsorption amount with increasing of ionic strength can be explained by considering the surface charge on the CHGE. Due to the salt effect, increasing ionic strength would increase the negative charge on the surface of the adsorbent. Increasing negative charge can effectively enhance the repulsion between adsorbent and dichromate (Cr⁶⁺ in basic water solution is found as Cr₂O₇²⁻) and decrease the Cr⁶⁺ adsorption. When NaCl concentration was higher than 0.3 mol L⁻¹, the increase of ionic strength would not induce the increase of negative charge, but would compress the double electric layer, neutralize negative charges on surface of the adsorbent, and thus weaken the repulsion between adsorbent and adsorbate ions [7], favoring the adsorption of Cr⁶⁺ onto the CHGE.

Author Contributions: Conceptualization, C.M.; methodology, C.M., V.M.; investigation, C.M., A.A. and V.M.; resources, C.M., V.M. and A.A.; writing—original draft preparation, C.M. and V.M.; writing—review and editing, C.M., V.M. and A.A.; project administration, A.A.; funding acquisition, A.A. All authors have read and agreed to the published version of the manuscript.

Funding: This research was funded by Spanish MINECO, grant number MAT2016-78155-C2-1-R, and by Government of The Principality of Asturias, grant number GRUPIN-IDI/2018/170.

Acknowledgments: Scientific-Technical Services of Oviedo University (Spain) for X-ray techniques, as well as the reviewers and editor for the manuscript revision.

Conflicts of Interest: The authors declare no conflict of interest.

References

- Jayabalakrishnan, R.M.; Mahimara, S. Adsorption of Hexavalent Chromium onto Raw Vermiculite Grades as a Function of Solution Concentration. *J. Appl. Sci. Res.* **2007**, *3*, 1262–1266.
- Sharma, Y.C.; Upadhyay, S.N.; Weng, C. Studies on an economically viable remediation of chromium rich waters and wastewaters by PTPS fly ash. *Colloid Surf. A Physicochem. Eng. Asp.* **2008**, *317*, 222–228. [[CrossRef](#)]
- Gupta, V.K.; Rastogi, A.; Nayak, A. Adsorption studies on the removal of hexavalent chromium from aqueous solution using a low cost fertilizer industry waste material. *J. Coll. Int. Sci.* **2010**, *342*, 135–141. [[CrossRef](#)] [[PubMed](#)]

4. Albadarin, A.B.; Mangwandia, C.; Al-Muhtaseb, A.H.; Walker, G.M.; Allen, S.J.; Ahmad, M.N.M. Kinetic and thermodynamics of chromium ions adsorption onto low-cost dolomite adsorbent. *Chem. Eng. J.* **2011**, *179*, 193–202. [[CrossRef](#)]
5. Dultz, S.; Jong-Hyok, A.; Riebe, B. Organic cation exchanged montmorillonite and vermiculite as adsorbents for Cr (VI): Effect of layer charge on adsorption properties. *Appl. Clay Sci.* **2012**, *67*, 125–133. [[CrossRef](#)]
6. Mulange wa Mulange, D.; Garbers-Craig, A.M. Stabilization of Cr (VI) from fine ferrochrome dust using exfoliated vermiculite. *J. Hazard. Mater.* **2012**, *223*, 46–52. [[CrossRef](#)]
7. Zhang, D.; Ying, M.A.; Feng, H.; Hao, Y. Adsorption of Cr(VI) from aqueous solution using carbon-microsilica: Composite adsorbent. *J. Chil. Chem. Soc.* **2012**, *57*, 964–968. [[CrossRef](#)]
8. Owalude, S.O.; Tella, A.C. Removal of hexavalent chromium from aqueous solutions by adsorption on modified groundnut hull. *Beni-Suef Univ. J. Basic Appl. Sci.* **2016**, *5*, 377–388. [[CrossRef](#)]
9. Jorfi, S.; Ahmadi, M.J.; Pourfadakari, S.; Jaafarzadeh, N.; Soltani, R.D.C.; Akbari, H. Adsorption of Cr (VI) by Natural Clinoptilolite Zeolite from Aqueous Solutions: Isotherms and Kinetic. *Pol. J. Chem. Technol.* **2017**, *19*, 106–114. [[CrossRef](#)]
10. Kan, C.; Ibe, A.H.; Rivera, K.K.P.; Arazo, R.A.; Luna, M.D.G. Hexavalent chromium removal from aqueous solution by adsorbents synthesized from groundwater treatment residuals. *Sustain. Environ. Res.* **2017**, *27*, 163–171. [[CrossRef](#)]
11. Marcos, C.; Rodríguez, I. Adsorption of trivalent chrome by thermo-exfoliated vermiculite. *Appl. Clay Sci.* **2014**, *90*, 96–100. [[CrossRef](#)]
12. Marcos, C.; Rodríguez, I. Thermoexfoliated commercial vermiculites for Ni²⁺ removal. *Appl. Clay Sci.* **2016**, *132*, 685–693. [[CrossRef](#)]
13. Mathieson, A.M.; Walker, G.F. Crystal structure of magnesium-vermiculite. *Am. Mineral.* **1954**, *39*, 231–255.
14. Calle, C.; de la Suquet, H. Vermiculite- Hydrous Phyllosilicates. In *Reviews in Mineralogy*; Bailey, S.W., Ed.; Mineralogical Society of America: Washington, DC, USA, 1988; Volume 19, pp. 455–496.
15. Marcos, C.; García, A.; Rodríguez, M.I.; Arango, Y.C. Behaviour of vermiculites with different composition at different temperatures. In *Proceedings of the 8th International Congress on Applied Mineralogy: Developments in Science and Technology, Águas de Lindóia, Brazil, 19–22 September 2004*; Pecchio, M., Andrade, F.R.D., D’Agostino, L.Z., Kahn, H., Sant’Agostino, L.M., Tassinari, M.M.M.L., Eds.; ICAM-BR: São Paulo, Brazil, 2004; pp. 627–629.
16. Argüelles, A.; Leoni, M.; Blanco, J.A.; Marcos, C. Structure and microstructure of Mg-vermiculite. *Z. Kristall. Suppl.* **2009**, *30*, 429–434.
17. Argüelles, A.; Leoni, M.; Blanco, J.A.; Marcos, C. Semi-ordered crystalline structure of the Sta. Olalla vermiculite inferred from X-ray powder diffraction. *Am. Mineral.* **2010**, *95*, 126–134. [[CrossRef](#)]
18. Suzuki, M.; Wada, N.; Hines, D.R.; Whittingham, M.S. Hydration states and phase transitions in vermiculite intercalation compounds. *Phys. Rev. B* **1987**, *36*, 2844–2851. [[CrossRef](#)] [[PubMed](#)]
19. Marcos, C.; Rodríguez, I. Expansion behaviour of commercial vermiculites at 1000 °C. *Appl. Clay Sci.* **2010**, *48*, 492–498. [[CrossRef](#)]
20. Marcos, C.; Arango, Y.C.; Rodríguez, I. X-ray diffraction studies of the thermal behaviour of commercial vermiculites. *Appl. Clay Sci.* **2009**, *42*, 368–378. [[CrossRef](#)]
21. Langmuir, I. The constitution and fundamental properties of solids and liquids. *J. Am. Chem. Soc.* **1916**, *38*, 2221–2295. [[CrossRef](#)]
22. Freundlich, H.M.F. Over the adsorption in solution. *J. Phys. Chem.* **1906**, *57*, 385–471.
23. Dubinin, M.M.; Radushkevich, L.V. The Dubinin-Radushkevich-Kaganer (DRK) equation. *J. Chem. Soc. Faraday Trans.* **1986**, *82*, 2473–2479.
24. Ho, Y.; Chiang, C. Sorption studies of acid dye by mixed sorbents. *Adsorption* **2001**, *7*, 139–147. [[CrossRef](#)]
25. Marcos, C. Structural changes in vermiculites induced by temperature, pressure, irradiation, and chemical treatments. In *Clay Science and Technology*; Morari Do Nascimento, G., Ed.; IntechOpen: London, UK, 2018.
26. Hamadi, N.K.; Chen, X.D.; Farid, M.M.; Lu, M.G.Q. Adsorption kinetics for the removal of Chromium(VI) from aqueous solution by adsorbents derived from used tyres and saw dust. *Chem. Eng. J.* **2001**, *84*, 95–101. [[CrossRef](#)]
27. Santamarina, J.C.; Klein, K.A.; Wangand, Y.H.; Prencke, E. Specific surface: Determination and relevance. *Can. Geotech. J.* **2002**, *39*, 233–241. [[CrossRef](#)]

28. Ziagova, M.; Dimitriadis, G.; Aslanidou, D.; Papaioannou, X.; Litopoulou Tzannetaki, E.; Liakopoulou-Kyriakides, M. Comparative study of Cd(II) and Cr(VI) biosorption on *Staphylococcus xylosus* and *Pseudomonas* sp. in single and binary mixtures. *Biores. Technol.* **2007**, *98*, 2859–2865. [[CrossRef](#)] [[PubMed](#)]
29. Malkoc, E.; Nuhoglu, Y.; Dundar, M. Adsorption of chromium (VI) on pomace—An olive oil industry waste: Batch and column studies. *J. Hazard. Mater. B* **2006**, *138*, 142–151. [[CrossRef](#)]
30. Sari, A.; Tuzen, M. Removal of Cr (VI) from aqueous solution by Turkish vermiculite: Equilibrium, thermodynamic and kinetic studies. *Sep. Sci. Technol.* **2008**, *43*, 3563–3581. [[CrossRef](#)]
31. Kimbrough, D.E.; Cohen, Y.; Winer, A.M.; Creelman, L.; Mabuni, C. A Critical Assessment of Chromium in the Environment. *Crit. Rev. Environ. Sci. Technol.* **1999**, *29*, 1–46. [[CrossRef](#)]
32. Lin, S.H.; Juang, R.S. Heavy metal removal from water by sorption using surfactant-modified montmorillonite. *J. Hazard. Mater.* **2002**, *92*, 315–326. [[CrossRef](#)]
33. Bhattacharya, A.K.; Mandal, S.N.; Das, S.K. Adsorption of Zn (II) from aqueous solution by using different adsorbents. *Chem. Eng. J.* **2006**, *123*, 43–51. [[CrossRef](#)]



© 2020 by the authors. Licensee MDPI, Basel, Switzerland. This article is an open access article distributed under the terms and conditions of the Creative Commons Attribution (CC BY) license (<http://creativecommons.org/licenses/by/4.0/>).